MODELLING A PLASMA SYSTEM FOR SOLITON AND SHOCKWAVES WITH A SPLITTING SCHEME AND A SECOND AND A THIRD ORDER HIGH RESOLUTION SCHEME

R.NAIDOO
Department of Mathematics
Durban University of Technology
P.O.BOX 1334,Durban,4001
South Africa
naidoor@dut.ac.za http://www.dut.ac.za

Abstract: - A splitting and a fully discrete second order and a third order semi discrete schemes are modified and adapted for a numerical solution of a hyperbolic system of a one dimensional electrostatic plasma fluid equation. Illustrations as to how the splitting and the NNT (fully discrete) and the semi-discrete (SD3) schemes capture the formation and evolution of ion acoustic solitons and shockwaves were performed. In this study we perform a comparison between a fully discrete NNT and the semi discrete SD3 high resolution schemes and the splitting scheme which is constructed for the first time for a one dimensional plasma systems in the present study. The results indicate that the splitting scheme demonstrates clear superiority over the NNT and SD3 schemes in the soliton solution where the numerical noise of the electron waves is reduced significantly. For the shock wave solution the NNT and SD3 schemes are similar to the splitting scheme but exhibit oscillations at the contact discontinuity. However the splitting scheme exhibit a smaller computational time than the NNT and SD3 schemes. It is thus advocated that in a one dimensional plasma system for solution and shockwaves simulations the splitting scheme and NNT /SD3 schemes be utilised respectively.

Key-Words: - **solitons,shockwaves,hyperbolic,plasma,split scheme,high resolution scheme**

1 Introduction

The central scheme algorithm such as the NNT and SD3 schemes is not sufficient to avoid oscillations especially for electron waves in the one dimensional plasmas. A more fundamental approach is required to understand the mechanism of the generation of over and undershoots in the numerical solutions of plasma fluids [2].

The approach towards high resolution upwind schemes consists in preventing the generation of oscillations by acting upon their production mechanism. Central schemes allow oscillations to appear and subsequently damped by artificial dissipation terms. The identification of upwind directions in the flux vector splitting methods is achieved with less effort than high resolution schemes leading to simpler more efficient schemes [7]. Hirsch [2] and Toro [7] points that the information concerning a flow field travels along characteristic lines. The upwind schemes are designed to numerically simulate more properly the direction of the propagation of information in a flow field along the characteristics curves. The central scheme does not always follow the proper flow of information through the flow fields [1]. In many cases central schemes draw numerical information outside the domain of dependence of a given grid point. This compromises accuracy of the solutions. Studies performed in plasma as in [3, 4], which are central schemes, indicates varying degrees of oscillations in the soliton and shockwave solutions. For an unsteady flow such as plasmas, which are common occurrences in power-electricity, laboratory and space situations, the value of the eigenvalue represents the velocity and the direction of the propagation of information along the characteristic lines. It would seem natural that a numerical scheme for solving the

flow equations should be consistent with the velocity and direction with which information propagates throughout the flow field. Hence the first time construction of a predictor-corrector splitting scheme for a numerical solution of the one dimensional plasma system in this study.

2 Problem Formulation

The model is considered to be in the general form

$$\frac{\partial u(x,t)}{\partial t}+\frac{\partial f(u)}{\partial x}=g(u(x,t)) \qquad (1)$$

which is the one dimensional hyperbolic system of partial differential equations? Here

$u(x,t)$ is the m-dimensional vector function, $f(u)$ is the flux vector and $g(u)$ is a continuous source vector, with x the single spatial coordinate and t is the temporal coordinate. Such equations can be used to model many physical systems including plasmas. Although high resolution schemes have been used on electrical plasma [4], numerical noise is still present in the numerical solutions.

Toro [7] indicates that upwind numerical methods should feature the discretisation of the equations on a mesh according to the direction of propagation of information on that mesh. The flux splitting methods achieves this by being simpler and more efficient [7]. The drawback is its reliance on the homogeneity property of (1).

The hyperbolic system (1) can be written as

$$\frac{\partial u(x,t)}{\partial t}+A\frac{\partial u}{\partial x}=g(u(x,t)) \qquad (2)$$

where $\frac{\partial f}{\partial u}=A$ is the Jacobian. If Λ is the diagonal matrix consisting of the eigenvalues then it is possible to write $A=K\Lambda K^{-1}$ where K is the transformation matrix with the eigenvectors. We may split the eigenvalues $\lambda_i=\lambda_i^+ +\lambda_i^-$ such that $\lambda_i^+>0, \lambda_i^-\le 0$ and Λ maybe split as $\Lambda=\Lambda^+ +\Lambda^-$ resulting in. $A^+=K\Lambda^+K^-$ and $A^-=K\Lambda^-K^-$ and $A=A^+ +A^-$ [2]

If the homogeneity property $f(u)=A(u)u$ then

$f=f^+ +f^-$, f^+ corresponds to the flux in the positive x direction with information being propagated from left to right by the positive eigenvalues opposite direction and f^- corresponds to the flux from right to left by negative eigenvalues. We can write

$f^+=A^+u$, $f^-=A^-u$.

However $\frac{\partial f^+}{\partial u}\neq A^+, \frac{\partial f^-}{\partial u}\neq A^-$ but $\frac{\partial f^+}{\partial u}$ has only positive eigenvalues and $\frac{\partial f^-}{\partial u}$ has only negative eigenvalues. Hence separating the characteristics and wave speeds according to the directions in the numerical scheme is met which is the objective of this study.

We now write the system (2) in conservation form although the eigenvalues are generally not equal to that of the Jacobian.A.

$$\frac{\partial u(x,t)}{\partial t}+\frac{\partial f^+}{\partial x}+\frac{\partial f^-}{\partial x}=g(u(x,t))[2] \qquad (3)$$

2.1 PLASMA FLUID SYSTEM

$$\frac{\partial n_k}{\partial t}+\frac{\partial (n_k v_k)}{\partial x}=0 \qquad (4)$$

$$m_k n_k\left(\frac{\partial v_k}{\partial t}+v_k\frac{\partial v_k}{\partial x}\right)+\frac{\partial p_k}{\partial x}=-q_k n_k\frac{\partial \phi}{\partial x} \qquad (5)$$

The set is closed by the equations of state (for ideal gases)

$$p_k n_k^{-\gamma_k}=cons\tan t \qquad (6)$$

and the Poisson's equation for the potential

$\frac{\partial^2\phi}{\partial x^2} = -4\pi\sum_{k=e,i} q_k n_k$. We write the equations as

$$\frac{\partial^2\phi}{\partial x^2} = u_1 - u_2 \equiv S(u) \tag{7}$$

The Poisson's equations were solved interatively as in [6].

We define field variables as

$u = [u_1, u_2, u_3, u_4]^T = [n_e, n_i, n_e v_e, n_i v_i]^T$ and the flux variables as

$$f = [f_1, f_2, f_3, f_4]^T = \left[u_3, u_4, \frac{u_3^2}{u_1} + \mu T_e u_1, \frac{u_4^2}{u_2} + T_i \frac{u_2^3}{u_{20}^2}\right]$$

and the source variables

$$g = [g_1, g_2, g_3, g_4] = \left[0, 0, \mu_e u_1 \frac{\partial\phi}{\partial x}, -u_2 \frac{\partial\phi}{\partial x}\right]$$

The index k=e(i) denotes electrons (ions) respectively and n_k, v_k, p_k, y_k, m_k and q_k are the respective component densities, flow velocities, partial pressures, adiabatic indices (=1 for isothermal electrons and =3 adiabatic ions), particle masses and charges and ϕ is the electric potential. T_e and T_i are the respective electron and ion temperatures and $\mu_e = \frac{m_e}{m_i}$ is the electron to ion mass ratio. The final equations are suitably normalized to time and spatial scales appropriate for the observation of ion-acoustic wave structures.[4] The Jacobian of the plasma fluid equations is given by

$$A = \begin{bmatrix} 0 & 0 & 1 & 0 \\ 0 & 0 & 0 & 1 \\ -\left(\frac{u_3}{u_1}\right)^2 + \mu_e T_e & 0 & 2\frac{u_3}{u_1} & 0 \\ 0 & -\left(\frac{u_4}{u_2}\right)^2 + 3T_i\frac{u_2^2}{u_{20}^2} & 0 & 2\frac{u_4}{u_2} \end{bmatrix} \tag{8}$$

The Euler homogeneity is only satisfied when $u_{20} = \sqrt{3}$ which is close to unity. It will be acceptable to use the homogeneity property in the plasma system.

The eigenvalues of A are: $\lambda_1, \lambda_2 = \frac{u_3}{u_1} \pm \sqrt{\mu_e T_e}$,

$$\lambda_3, \lambda_4 = \frac{u_4}{u_2} \pm \frac{u_2}{u_{20}}\sqrt{3T_i} \tag{9}$$

with corresponding eigenvectors

$$W_1, W_2 = \left[\frac{1}{\lambda_1}, 0, 1, 0\right]^T, \left[\frac{1}{\lambda_2}, 0, 1, 0\right]^T$$
$$W_3, W_4 = \left[0, \frac{1}{\lambda_3}, 0, 1\right]^T, W_4 = \left[0, \frac{1}{\lambda_4}, 0, 1\right]^T \tag{10}$$

There are four distinct eigenvectors and corresponding eigenvalues which are linearly independent. Hence the Jacobian is diagonalizable.

We define the matrix K as the eigenvector matrix

$$K = \begin{bmatrix} \frac{1}{\lambda_1} & \frac{1}{\lambda_2} & 0 & 0 \\ 0 & 0 & \frac{1}{\lambda_3} & \frac{1}{\lambda_4} \\ 1 & 1 & 0 & 0 \\ 0 & 0 & 1 & 1 \end{bmatrix}$$

$$K^{-1} = \begin{bmatrix} -\frac{\lambda_1\lambda_2}{\lambda_1 - \lambda_2} & 0 & \frac{\lambda_1}{\lambda_1 - \lambda_2} & 0 \\ \frac{\lambda_1\lambda_2}{\lambda_1 - \lambda_2} & 0 & -\frac{\lambda_2}{\lambda_1 - \lambda_2} & 0 \\ 0 & -\frac{\lambda_3\lambda_4}{\lambda_3 - \lambda_4} & 0 & \frac{\lambda_3}{\lambda_3 - \lambda_4} \\ 0 & \frac{\lambda_3\lambda_4}{\lambda_3 - \lambda_4} & 0 & -\frac{\lambda_4}{\lambda_3 - \lambda_4} \end{bmatrix} \tag{11}$$

We define the diagonal matrix as

$$\Lambda=\begin{bmatrix} \frac{u_3}{u_1}+\sqrt{\mu_e T_e} & 0 & 0 & 0 \\ 0 & \frac{u_3}{u_1}-\sqrt{\mu_e T_e} & 0 & 0 \\ 0 & 0 & \frac{u_4}{u_2}+\frac{u_2}{u_{20}}\sqrt{3T_i} & 0 \\ 0 & 0 & 0 & \frac{u_4}{u_2}-\frac{u_2}{u_{20}}\sqrt{3T_i} \end{bmatrix}$$

$$=\begin{bmatrix} \lambda_1 & 0 & 0 & 0 \\ 0 & \lambda_2 & 0 & 0 \\ 0 & 0 & \lambda_3 & 0 \\ 0 & 0 & 0 & \lambda_4 \end{bmatrix} \qquad (12)$$

and $A = K\Lambda K^{-1}$

$$\Lambda^+ = \begin{bmatrix} \lambda_1 & 0 & 0 & 0 \\ 0 & 0 & 0 & 0 \\ 0 & 0 & \lambda_3 & 0 \\ 0 & 0 & 0 & 0 \end{bmatrix} \quad \Lambda^- = \begin{bmatrix} 0 & 0 & 0 & 0 \\ 0 & \lambda_2 & 0 & 0 \\ 0 & 0 & 0 & 0 \\ 0 & 0 & 0 & \lambda_4 \end{bmatrix} \qquad (13)$$

$$A^+ = K\Lambda^+ K^{-1} = \begin{bmatrix} -\frac{\lambda_1\lambda_2}{\lambda_1-\lambda_2} & 0 & \frac{\lambda_1}{\lambda_1-\lambda_2} & 0 \\ 0 & -\frac{\lambda_3\lambda_4}{\lambda_3-\lambda_4} & 0 & \frac{\lambda_3}{\lambda_3-\lambda_4} \\ -\frac{\lambda_1^2\lambda_2}{\lambda_1-\lambda_2} & 0 & \frac{\lambda_1^2}{\lambda_1-\lambda_2} & 0 \\ 0 & -\frac{\lambda_3^2\lambda_4}{\lambda_3-\lambda_4} & 0 & \frac{\lambda_3^2}{\lambda_3-\lambda_4} \end{bmatrix} \qquad (14)$$

$$A^- = K\Lambda^- K^{-1} = \begin{bmatrix} \frac{\lambda_1\lambda_2}{\lambda_1-\lambda_2} & 0 & -\frac{\lambda_2}{\lambda_1-\lambda_2} & 0 \\ 0 & \frac{\lambda_3\lambda_4}{\lambda_3-\lambda_4} & 0 & -\frac{\lambda_4}{\lambda_3-\lambda_4} \\ \frac{\lambda_1\lambda_2^2}{\lambda_1-\lambda_2} & 0 & \frac{\lambda_2^2}{\lambda_1-\lambda_2} & 0 \\ 0 & \frac{\lambda_3\lambda_4^2}{\lambda_3-\lambda_4} & 0 & -\frac{\lambda_4^2}{\lambda_3-\lambda_4} \end{bmatrix} \qquad (15)$$

$$F^+ = A^+U = \begin{bmatrix} \frac{u_3\lambda_1}{\lambda_1-\lambda_2} - \frac{u_1\lambda_1\lambda_2}{\lambda_1-\lambda_2} \\ \frac{u_4\lambda_3}{\lambda_3-\lambda_4} - \frac{u_2\lambda_3\lambda_4}{\lambda_3-\lambda_4} \\ \frac{u_3\lambda_1^2}{\lambda_1-\lambda_2} - \frac{u_1\lambda_1^2\lambda_2}{\lambda_1-\lambda_2} \\ \frac{u_4\lambda_3^2}{\lambda_3-\lambda_4} - \frac{u_2\lambda_3^2\lambda_4}{\lambda_3-\lambda_4} \end{bmatrix} \qquad (16)$$

$$F^- = A^-U = \begin{bmatrix} -\frac{u_3\lambda_2}{\lambda_1-\lambda_2} + \frac{u_1\lambda_1\lambda_2}{\lambda_1-\lambda_2} \\ -\frac{u_4\lambda_4}{\lambda_3-\lambda_4} + \frac{u_2\lambda_3\lambda_4}{\lambda_3-\lambda_4} \\ \frac{u_1\lambda_1\lambda_2^2}{\lambda_1-\lambda_2} + \frac{u_3\lambda_2^2}{\lambda_2-\lambda_1} \\ -\frac{u_4\lambda_4^2}{\lambda_3-\lambda_4} + \frac{u_2\lambda_4^2\lambda_3}{\lambda_3-\lambda_4} \end{bmatrix} \qquad (17)$$

2.2 NUMERICAL MODELS

2.2.1 SPLITTING SCHEME

In (3) $\frac{\partial f^+}{\partial x}$ can be replaced by a backward difference since f^+ is associated only with information coming from upstream of grid point (i,j) ie. it corresponds with flux in the positive x direction with information being propagated

from left to right by positive eigenvalues λ_1 and λ_3. Again in (3) $\frac{\partial f^-}{\partial x}$ can be replaced by a forward difference since f^- corresponds to a flux in the negative x direction, with information being propagated from right to left by the negative eigenvalues λ_2 and λ_4 and is associated with information coming from down stream of grid (i,j). Using the aforementioned phenomena the flux splitting method is designed to account for the physically proper transfer of information throughout the flow.

Taking the flow from (i,j) a predictor-corrector scheme is designed as follows:

$$\bar{u}_i = u_0 - \lambda\left(f_i^+ - f_{i-1}^+ + f_{i+1}^- - f_i^-\right) + \Delta t g_i \text{ - predictor} \quad (18)$$

where u_0 is the initial value and $\lambda = \frac{\Delta t}{\Delta x}$

$$u_{1i} = \bar{u}_i - \lambda\left(\bar{f}_i^+ - \bar{f}_{i-1}^+ + \bar{f}_{i+1}^- - \bar{f}_i^-\right) + \Delta t \bar{g}_1 \text{ - corrector}$$

2.2.2 NNT SCHEME

We employ the modified Nessyahu and Tadmor numerical scheme [2,3,4]. The second order formula is given as follows:

$$\bar{u}_j^{n+1} = \frac{1}{4}\left[\bar{u}_{j+1}^n + 2\bar{u}_j^n + \bar{u}_{j-1}^n\right] - \frac{1}{16}\left[u_{xj+1}^n - u_{xj-1}^n\right] - \frac{1}{8}\left[u_{xj+\frac{1}{2}}^{n+1} - u_{xj-\frac{1}{2}}^{n+1}\right] + \frac{\Delta t}{8}\left[g\left(u_{j+1}^n\right) + 2g\left(u_j^n\right) + g\left(u_{j-1}^n\right)\right] + \frac{\Delta t}{8}\left[g\left(u_{j+1}^{n+1}\right) + 2g\left(u_j^{n+1}\right) + g\left(u_{j-1}^{n+1}\right)\right] - \frac{\lambda}{4}\left[\left(f_{j+1}^n - f_{j-1}^n\right) + \left(f_{j+1}^{n+1} - f_{j-1}^{n+1}\right)\right] \quad (19)$$

where $\bar{u}_j^n$ is the cell average at $x_j, \Delta x = x_{j+1} - x_j, \Delta t = t^{n+1} - t^n$ and $\lambda = \frac{\Delta t}{\Delta x}$ is the CFL value.

As in shock calculations we shall employ the min-mod derivatives [5]:

$$u_{xj-\frac{1}{2}}^{n+1} = MM\left(\Delta u_j^{n+1}, \Delta u_{j-1}^{n+1}\right), u_{xj+\frac{1}{2}}^{n+1} = MM\left(\Delta u_{j+1}^{n+1}, \Delta u_j^{n+1}\right)$$

where the nonlinear limiter MM is defined by

$$\mathrm{MM}(s_1, s_2, \ldots) = \begin{cases} \min\{s_j\} \text{ if } s_j > 0 \forall j \\ \max\{s_j\} \text{ if } s_j < 0 \forall j \\ 0 \text{ otherwise} \end{cases}$$

And where after some simplification:

$$\begin{aligned} \Delta u_j^{n+1} &= \bar{u}_{j+\frac{1}{2}}^{n+1} - \bar{u}_{j-\frac{1}{2}}^{n+1} \\ &= \frac{1}{2}\left[\bar{u}_{j+1}^n - \bar{u}_{j-1}^n\right] - \frac{1}{8}\left[u_{xj+1}^n - 2u_{xj}^n + u_{xj-1}^n\right] - \frac{\lambda}{2}\left[f_{j+1}^{n+1} - 2f_j^{n+1} + f_{j-1}^{n+1} + f_{j+1}^n - 2f_j^n + f_{j-1}^n\right] \\ &= \frac{\Delta t}{4}\left[g\left(u_{j+1}^{n+1}\right) - g\left(u_{j-1}^{n+1}\right) + g\left(u_{j+1}^n\right) - g\left(u_{j-1}^n\right)\right] \end{aligned} \quad (20)$$

Here again the $u_{xj} = \mathrm{MM}\left(u_{j+1} - u_j, u_j - u_{j-1}\right)$

Also useful in our applications is the more accurate UNO derivative [5]

$$u_{xj} = \mathrm{MM}\left(u_j - u_{j-1} + \frac{1}{2}\mathrm{MM}\left(u_j - 2u_{j-1} + u_{j-2}, u_{j+1} - 2u_j + u_{j-1}\right), u_{j+1} - u_j - \frac{1}{2}\mathrm{MM}\left(u_{j+1} - 2u_j + u_{j-1}, u_{j+2} - 2u_{j+1} + u_j\right)\right).$$

To apply the scheme, which is implicit in time, we use the predictor given in [4]

$$u^{n+1} = u^n + \Delta t\left[g\left(u^n\right) - \frac{1}{\Delta x} f_x^n\right] \quad (21)$$

where the flux derivative $\frac{1}{\Delta x} f_x^n$ are at the indicated time level n and can be evaluated using the MM function or calculated from the explicit form of $f(u)$.

2.3 SD3 SCHEME

The semi-discrete numerical scheme is outlined in [3]. In applying this method we employ uniform spatial and temporal grids with spacings, $\Delta x = x_{j+1} - x_j$;

$\Delta t = t^{n+1} - t^n$ (with j and n being suitable integer indices) together with the semi-discrete scheme ("SD3")

$$\frac{d\bar{u}_j}{dt} = -\frac{1}{2\Delta x}\left[f\left(u^+_{j+\frac{1}{2}}(t)\right) + f\left(u^-_{j-\frac{1}{2}}(t)\right) - f\left(u^+_{j-\frac{1}{2}}(t)\right) - f\left(u^-_{j-\frac{1}{2}}(t)\right)\right]$$

$$-\frac{a_{j+\frac{1}{2}}(t)}{2\Delta x}\left[u^+_{j+\frac{1}{2}}(t) - u^-_{j+\frac{1}{2}}(t)\right] - \frac{a_{j-\frac{1}{2}}(t)}{2\Delta x}\left[u^+_{j-\frac{1}{2}}(t) - u^-_{j-\frac{1}{2}}(t)\right] + g(u_j(t)) \quad (22)$$

We note in particular that the solution is updated by fitting on already computed or known cell average values $\left\{\bar{U}_j^n\right\}$ at time level n, piecewise polynomials of degree two on cells of size Δx central at x_j namely

$P_j(x,t^n) = A_j + B_j(x - x_j) + C_j(x - x_j)^2$

Where the constants are $(A_j \ldots\ldots)$ are specified later.

Here $u^+_{j\pm\frac{1}{2}} := P_{j+1}(x_{j\pm\frac{1}{2}}, t^n); u^-_{j\pm\frac{1}{2}} := P_j\left(x_{j\pm\frac{1}{2}}, t^n\right)$ (23)

$$a^n_{j\pm\frac{1}{2}} = \max\left(\rho\left(\frac{\partial f}{\partial u}(u^-_{j\pm\frac{1}{2}}(t))\right), \rho\left(\frac{\partial f}{\partial u}(u^+_{j\pm\frac{1}{2}}(t))\right)\right) \quad (24)$$

Where the forms (24) are respectively the left and right intermediate values at $x_{j+\frac{1}{2}}$ and $\rho(.)$ denotes the spectral radii of the respective flux Jacobian, defining the maximum local propagation speeds $a^n_{j\pm\frac{1}{2}}$.

STABILITY

3.1 NNT AND SD3 SCHEMES

The NNT stability has been calculated using Roe's stability formula [2]. The linear stability analysis of the NNT/SD3 scheme indicates that it should remain stable under CFL condition $\Lambda_m \frac{\Delta t}{\Delta x} \le 0.01$, where Λ_m is the spectral radius of the flux Jacobian. This is stronger than that for the NNT/SD3 scheme in [3] for electrostatic simulations.

We take $\Delta x = 0.1, \Delta t = 0.001$. The CFL value can be calculated as

$$CFL = \frac{\Delta t}{\Delta x} = \frac{0.001}{0.1} = 0.01$$

3.2 SPLITTING SCHEME

Using the amplification factor G from the Von Neumann analysis

$$G - 1 = -2\tau(f_u^+ - f_u^-)\sin^2\frac{\vartheta}{2} - i\tau(f_u^+ + f_u^-)\sin\vartheta$$

[2]

After some simplification by Hirsch[2] demonstrated that the stability of (18) can be written as $\tau|\lambda|_{max} \le 1$ where $|\lambda|_{max}$ represent the maximum eigenvalue of the Jacobian A in (2).

All boundary conditions were reflective.

Neumann homogeneous ($\frac{\partial u}{\partial x} = 0$) [1].

4. INITIAL CONDITIONS:

4.1 SOLITON SOLUTION

Plasma system perturbation NNT and Splitting Waves are set as follows:

$$n_e(n_i) = 1 + e^{-0.5x^2}, -100 \le x_c \le 100$$
$$n_e(n_i) = 1 \, elsewhere$$
$$v_e(v_i) = 0 \; \forall x$$

4.2 SHOCK SOLUTION:

4.2.1 RIEMANN SHOCK TUBE

PROBLEM:

It is the local solution of the Riemann problem which involves the solution of the Euler equations which are nonlinear. An initial shockwave is set as follows:

Where $\rho_{1/2}$ is the left and right density respectively and $m_{1/2}$ are the left and right momentum respectively for the shockwave. The following are SD3 shock initial conditions.

$$\begin{cases} n_{e(i)} = 2.5 \\ n_{e(i)} v_{e(i)} = 1.0 \end{cases}, x_c < 100 \; grids$$

$$\begin{cases} n_{e(i)} = 1.0 \\ n_{e(i)} v_{e(i)} = 0.4 \end{cases}, x_c > 100 \; grids$$

The following are initial conditions for NNT initial conditions.

$$\begin{cases} \rho_1 = 2 \\ m_1 = 0 \\ \rho_2 = 1 \\ m_2 = 0 \end{cases}$$

5. Problem Solution

TABLE 1: COMPUTATION TIME:

SCHEME	COMPUTATION TIMES
SPLITTING	105
NNT	321
SD3	679

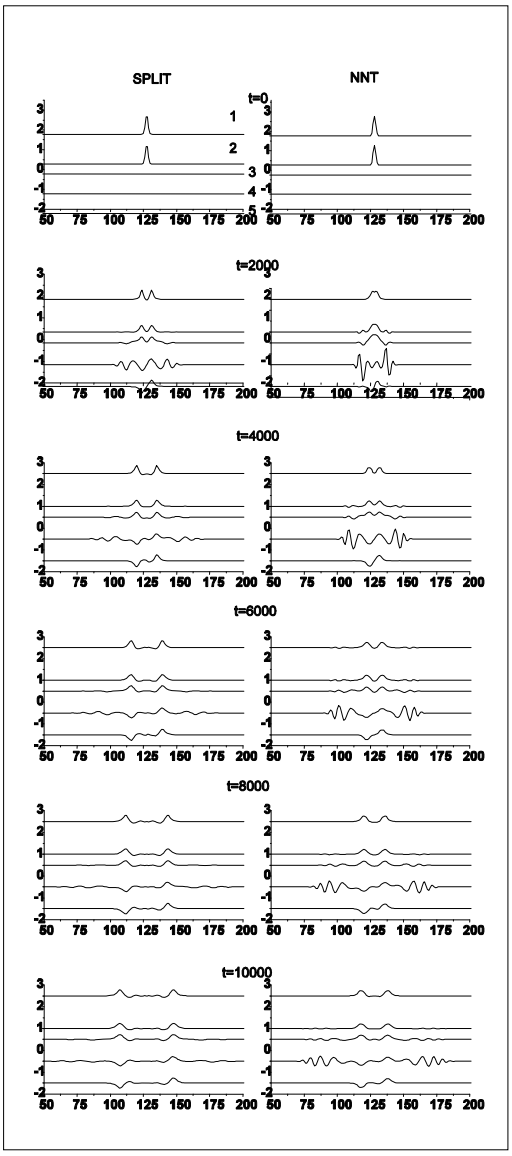

Fig1: Solitons: 1~n_i+1.5(ion density), 2~n_e(electron density), 3~potential+0.5, 4~v_e -0.5 (velocity of electrons),5~v_i -1.5 (ion velocity). $\Delta t = 0.001$,$\Delta x = 0.1$,t=time in 1000 units.

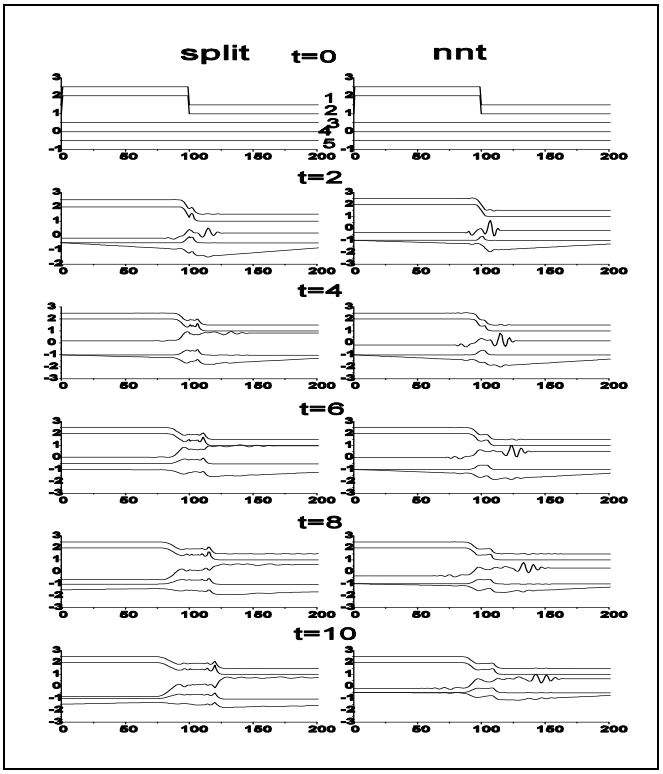

Fig2: Shockwaves: 1~electron density, 2~ ion density, 3~electron momentum

4~ionmomentum, 5~potential $\Delta t = 0.001$,

$\Delta x = 0.1$,t=time in 1000 units

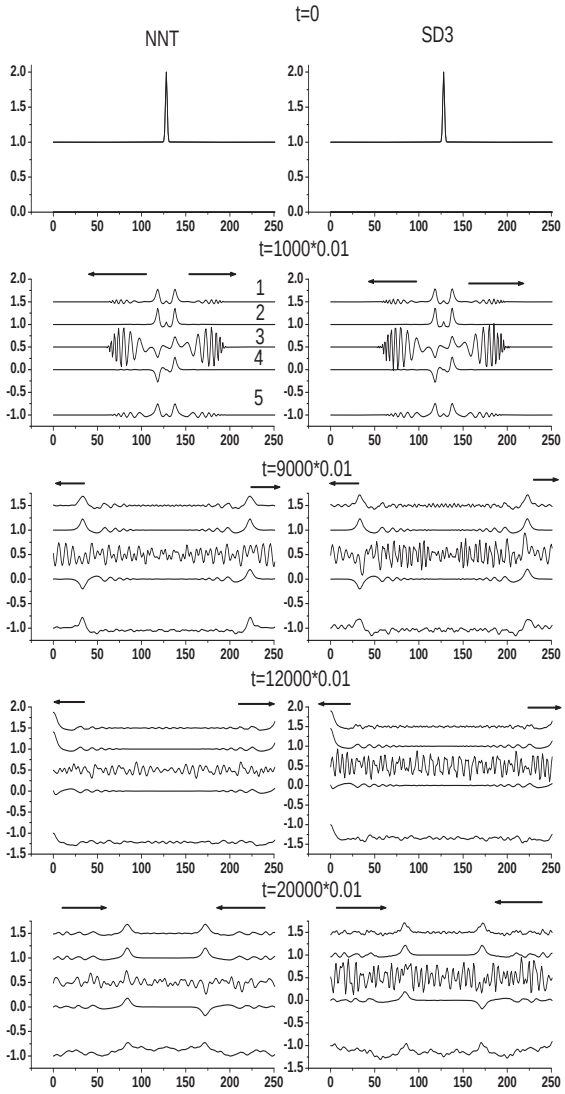

Fig 3: Formation and time evolution of a Gaussian-perturbation induced solitons in a plasma fluid with a NNT and SD3 schemes. Here the curve labelled
$1 \sim n_e + 0.5, 2 \sim n_i\ 3 \sim v_e + 0.5, 4 \sim v_i, 5 \sim \phi$ -1
where $n_e(n_i)$ is the electron/ion density, $v_e(v_i)$ is the electron/ion flow velocity, ϕ is the electrostatic potential all in normalised units.

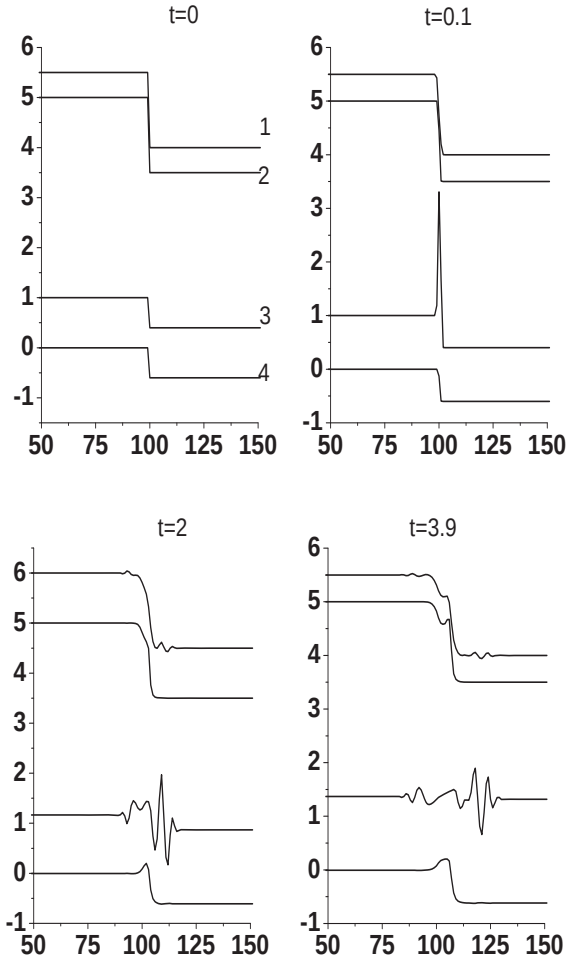

Fig 4: SD3 Shockwaves. Here the curve labelled
$1 \sim n_e + 3.5,\ 2 \sim n_i + 2.5,\ 3 \sim v_e, 4 \sim v_i - 1$
where $n_e(n_i)$ is the electron/ion density, $v_e(v_i)$ is the electron/ion flow velocity, all in normalised units.

6 CONCLUSION

In figure 1 we see that the splitting scheme for numerically integrating a system of fluid equations can be successfully applied to study important nonlinear wave structures, in

particular, solitons and shockwaves in a plasma fluid.

The computational times in the table above indicates that the NNT scheme was much larger than the splitting scheme approximately three times. The soliton wave speed is slower than the splitting scheme indicating that the NNT scheme experiences a degree of damping.

The NNT scheme exhibits numerical noise (see wave number 4 in figure 1) especially in the electron waves whilst in the spitting scheme the electron wave's numerical noise seem to have been eliminated. The splitting scheme is able to contain spurious oscillations due to boundary reflections.

Furthermore as time increases the NNT becomes less stable whilst the splitting scheme is stable over long time evolution of ion acoustic solitons in a plasma fluid (See Figure1 and Figure 3).

Hence the splitting scheme is computationally less expensive and more stable than the NNT scheme in the soliton simulation.

It is recommended that the splitting scheme is a better option as stable modelling engines in nonlinear plasma soliton studies.
In figure 2 the shock wave solution for the split scheme exhibits mild oscillations at the contact regions (see wave number 3). As time progresses the shockwaves, contact waves and rarefaction waves becomes conspicuous for both schemes. The shockwaves travel faster in the split scheme than the NNT scheme. However the NNT scheme exhibits more accurate shockwave profile.

In figure 3 we observe that the solitons exhibited by the NNT scheme exhibits much less numerical oscillations than the SD3 scheme.
In figure 4 we observe the SD3 shockwaves moving to the left and right together with the contact discontinuity moving to the right. Sharp electron waves are observed at the discontinuity whilst the ion waves remains relatively smooth. For larger times the density of the electron and ion waves tend to break-up at the discontinuity due to the fluctuation of the electric fields. The density and momentum propagation tend to be stable as time progresses.
It is there recommended that the split scheme is better than the high resolution schemes in that it stabilises the electron waves by reducing the numerical noise. For shockwaves the split scheme, SD3 and NNT schemes exhibited the satisfactory waves although the high resolution schemes fare well in other examples such as gases [2].

References:

[1].Anderson,J.D. 1982 Computational Fluid Dynamics. McGraw-Hill, New York.

[2]Hirsch,C. Numerical Computation of Internal and External Flows,vols 1 and 2 Wiley, Sussex 1997

[3]Naidoo,R and Baboolal,S. (2004) Adaptation and assessment of a high resolution semi-discrete numerical scheme for hyperbolic systems with source terms and stiffness,Fut.Gen.Comput.Sys.20,465

[4]Naidoo,R and Baboolal,S. (2003) Numerical integration of the plasma fluid equations with a modification of the second-order Nessyahu-Tadmor central scheme and soliton modelling. Mathematics and Computers in Simulation 69 (2005) 457-466

[5]Nessyahu H. and Tadmor,E. (1990): Non-oscillatory central differencing for hyperbolic conservation laws, J.Comput.Phys.87,408

[6] Ren-Chuen Chen. An Iterative Method for Finite-Element Solutions of the Nonlinear Poisson-Boltzmann Equation. WSEAS TRANSACTIONS on COMPUTERS pp 165-173March 5, 2008

[7]Toro,E.F. (1999) Riemann Solvers and Numerical Methods for Fluid Dynamics , Springer,London